Investigation of three events of solar parameters and Interplanetary Coronal Mass ejections during the maximum phase of solar cycle 24

M. S. Dhaiya[1], S. S. Bidhu[2], A. Iren Sobia[3]

[1] Research scholar (Reg. No:20213092132011), Department of Physics and Research Centre, Muslim Arts College, Thiruvithancode – 629174, Tamilnadu, India.
Affiliated to Manonmaniam Sundaranar University, Abishekapatti, Tirunelveli – 627012, Tamil Nadu, India
deenamasha@gmail.com

[2] Assistant Professor, Department of Physics and Research Centre, Nanjil Catholic College of Arts and Science, Kaliyakkavilai - 695502, Tamilnadu, India.

[3] Assistant Professor, Department of Physics and Research Centre, Muslim Arts College, Thiruvithancode - 629174, Tamilnadu, India.

(Submitted on 18 November 2023; Accepted on 26 January 2024)

Abstract. This paper analyzes the Three events of Solar Parameters and Interplanetary Coronal Mass Ejections in the maximum phase of Solar Cycle 24 and focuses on the magnetic activity of interplanetary coronal mass ejection during the solar cycle 24. We investigate the magnetic field magnitude (B), Proton temperature (Tp), Proton density (Np). From this study, we find the highest peak of IP (Interplanetary) shocks on disk center MC (Magnetic cloud) events during the solar cycle 24 and also we investigate the magnetic activity of the solar cycle. In this study, we find that the ACE spacecraft shows the fastest coronal mass ejection and highest interplanetary shock wave on solar cycle 24. It is important to note that extreme events can happen at any time during a cycle. In solar cycle 24, from July 13, 2012 to July 15, 2012 largest storm occurred because the magnetic field was -52nT and linear speed was 1500 $\mathrm{km\,s^{-1}}$ observed.

Key words: Interplanetary Coronal Mass Ejection, Magnetic activity, Magnetic cloud, IP shocks

Introduction

The Sun is the main source of heat and light in the solar system. The number of sunspots that can be seen on the Sun's surface varies over the duration of an 11-year solar cycle. Along with other factors, it has something to do with the solar cycle, magnetic field, coronal mass ejections, solar outbursts and radio emission.

The large amount of ionized plasma that can come out of the upper atmosphere of the Sun is called a Coronal Mass Ejection (CME). CMEs are very important events for the Sun. The view of the White-light corona graph field is different and extremely bright, showing that the CME was moving away on the timescale of minutes to hours (Munro et al., 1979).

The CME comes from corona of the Sun. The fastest mode shocks speed up the charged particles and also produce very powerful geomagnetic storm. The most energetic phenomenon in the heliosphere are interplanetary coronal mass ejections (ICMEs) and is detected in the corona graph. This presents an overview of the observational features of ICMEs in respect to the normal solar wind and their ancestor CMEs.

We looked at how the speed of the CMEs, which propel the shocks towards the Sun and into the IP medium, affected the IP shocks mentioned by Gopalswamy et al. (2010). We discover that SC/SIs were responsible for

nearly 91 percentage of IP shocks. The CMEs connected to sudden commencement(SCs) and sudden impulses(SIs) have an average speed of 1015 $\mathrm{km\,s^{-1}}$. This is roughly double the speed of a conventional CME.

It is well known that CMEs, which are large-scale structures, are connected to coronal slow/fast streamers, coronal gaps, and other CMEs. Advanced radio emission, particle acceleration, solar wind bulk flow speed, proton density, CME deflection, and proton temperature are a few of these interactions' prominent consequences. CMEs can deviate from the Sun-Earth axis and still strike the planet. The Sun-Earth line may finally be struck by CMEs that have been diverted, resulting in powerful geomagnetic storms.

The CMEs are made up of two occurrences: halo and partial halo events with a width larger than 120°. Because of how they appear in corona graph photos during the solar cycle's maximum and rising phases, these CMEs occurred throughout the solar cycle's rising and maximum phases, which lasted from 2009 to 2019. Because of how they appear in corona graph photos, coronal mass ejections directed at Earth are referred to as "halo events". The Sun looks to be being enriched by the growing cloud of an Earth-directed CME, which is encircling our star. CMEs with a halo have an apparent angular width of 360 degrees. In contrast to limb halos, which have an apparent angular width between 45°and 90°, CMEs have an apparent angular width between 120°and 360°.

Based on data from the Advanced Composition Explorer (ACE) spacecraft (Richardson & Cane, 2010) and numerous thorough ICME catalogues, measurements are provided. It is impossible to analyse ICMEs using a single, entirely objective method (Huttunen et al., 2005), hence some subjective judgments may influence how ICMEs are detected and how accurately their boundaries are specified. Chi (2016) found that despite some variances, the results of the RC and Chi catalogues are comparable.

To carry out our current studies, first ICMEs in the background solar wind must be identified according to a number of criteria, such as increased magnetic field strength, smoothly changing field direction, low proton temperature, etc. (Zurbuchen & Richardson, 2006; Wu & Lepping, 2011; Song & Yao, 2020). Then, each ejecta should be given an MC. The progressive change in field direction is the characteristic of MCs that is most noticeable. Here, in order to separate the concerns of ICME identification and statistics and to narrow the emphasis of our investigation, we decided to use the ICME catalogue offered by the specialists in this field instead of recognising the events ourselves.

Magnetic clouds are huge interplanetary flux ropes that grow as they travel through the solar wind from the Sun. We look at how in situ data and magnetic cloud models, which are represented as cylindrical shape magnetic flux ropes with expansion, correspond. We continue our earlier investigation of the Rise, Maximum, and Declining phases of solar cycle 24 in this paper. Because each ICME is located nearer to the disk's core, both the Data section and the Data Analysis Method were assessed.

1 Data Selection and Method of Analysis

The data used in this study are taken from ACE. The IP CMEs and Magnetic clouds we examined are listed at the below link[4]. Richardson & Cane (2010) and the MCs of cycle 24 published before (Gopalswamy et al., 2008; Lepping et al., 2015) are used. We use proton temperature and magnetic field data from the ACE' MAG-SWEPAM level 64-sec averages[5]. For each ICME, there is a corresponding CME observed by the Large Angle and Spectrometric Coronagraph (LASCO) (Brueckner et al., 1995) on board the Solar and Heliospheric Observatory (SOHO) mission.

2 Result and Discussion

2.1 Magnetic cloud during solar cycle 24

Table 1. Number of Magnetic cloud during 24^{th} solar cycle

Year	MC count
2008	04
2009	12
2010	17
2011	36
2012	44
2013	35
2014	24
2015	03
2016	18
2017	12
2018	11
2019	10

SOHO has recorded 255 MCs during Solar Cycle 24. We began with the MC events that were reported between December 2008 and December 2019. Due to the Sun's low activity and small range of CMEs, Solar Cycle 24, 2008, only saw four CMEs. Due to the Sun's activity being higher than other occurrences in solar cycle 24 in 2012, 44 MCs were detected by the LASCO sensor on board SOHO. The MCs with the highest speed and largest overall magnitudes in this solar cycle are located nearer to the centre of the solar disc, which makes little sense when hyphenated across lines.

2.2 ICME Identification for Selected Event

Gopalswamy (2010) used the following data to identify the MCs in charge of IP shocks: (Stone et al., 1998) employed the ACE's magnetic field magnitude

[4] *www.srl.caltech.edu/ACE/ASC/DATA/ level3/icmetable2.htm*
[5] *www.srl.caltech.edu/ACE/ ASC/level2/lvl2DATA$_M$AG − SWEPAM.html*

Table 2. Disk center MC Events during the three phases of solar cycle 24

Phase	Shock		MC	
	Date	Time(UT)	Start time(UT)	Duration(h)
Rising phase	07/02/10	1425	07/1800	28
	12/02/10	0413	02/0800	19
	07/03/11	1542	06/0900	45
	05/06/11	0052	05/0200	17
	05/08/11	1920	05/0500	09
	09/09/11	1216	10/0300	26
	26/09/11	1308	26/2000	31
	25/10/11	0904	24/2200	18
	29/11/11	0256	29/0000	08
	29/11/12	0412	29/2200	15
Maximum phase	17/06/12	0120	16/2300	08
	15/07/12	0720	15/0600	13
	03/09/12	1156	04/1100	45
	07/03/13	0740	17/1000	15
	02/10/13	0420	02/2300	09
	08/10/13	0216	09/0900	23
	09/11/13	6504	08/2200	39
	08/12/13	0216	08/0100	09
	16/02/14	0400	16/0500	33
	06/04/14	0212	05/2200	11
	20/08/14	1104	19/1600	31
	12/09/14	1812	12/2200	37
	23/12/14	1045	22/0400	28
	17/03/15	1336	17/1300	13
	20/09/15	1536	21/0800	16
Declining phase	19/07/16	0700	19/1500	08
	24/07/16	1500	25/1600	25
	12/10/16	2212	13/0600	08
	08/09/17	1100	10/2100	38
	30/06/18	2000	02/1000	14
	16/05/19	2100	18/0800	11

(B) and its Y and Z components (By, Bz), solar wind bulk flow speed (V), proton temperature (Tp), and proton density (Np) data in GSE coordinates.

The relationship between ICMEs and the associated CMEs detected by SOHO/LASCO was made by looking at all CMEs that took place during a window of 0.5 to 5 days prior to the shock arrival time at 1 AU (Gopalswamy, 2010).

Figures 2, 3, and 4 each depict one instance of an ICME being driven by shock: an MC on July 15, 2012, at 07:20 UTC. The MC event took place during the decline stage. Whether the ICME signal is present or not, it is clear that the Tp is high in the sheath region between the shock and the start of the ejecta (this region is typical of all shocks). Remember that the Tp depression and the bulk of the other traits persist past the designated MC period, which may suggest that there were one or more non-MCs following the first MC.

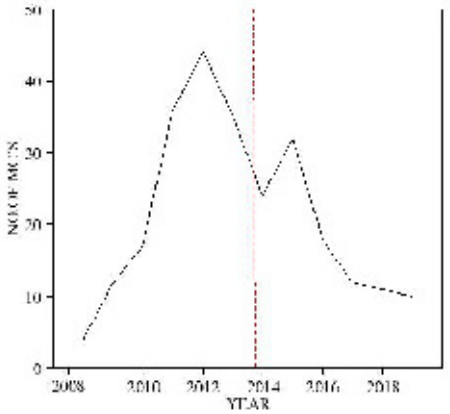

Fig. 1. Number of magnetic cloud during 2008-2019, X-axis indicates year and Y-axis indicates Number of MC. The data is taken from ACE. The Red grid line indicates the large number of MCs.

There are typically a few small variances in the identification of ICME limits by different authors, although these differences only last a few hours.

CME's heliospheric equivalents are ICMEs. When they are seen on corona graphs, CMEs are sometimes referred to as ICMEs. In Table 2, the first column shows the three phases data of solar cycle 24 and the three phases are rising phase, maximum phase and declining phase. The second column and the third column shows the IP shock occurring date and time. The time is denoted in Universal time. Fourth and fifth column shows the MC start time and duration and in Table 3, the first column shows the three phases data of solar cycle 24. Second and third column shows the CME event starting time in Universal time and duration. Fourth column shows the CME speed in kilometre per second. The fifth column shows the Measurement position angle (MPA). In this Table we take three important ICME and MC events, on that day the solar wind emitted from the Sun's outer atmosphere was very fast, so we have the giant magnetic flux rope, therefore IP shock reaches the high peak and also a more active MC was occurred.

2.3 ICME and MC event on 15 July 2012

The ICME shock's surface location is S17 W08, and it lasted from July 14 at 17:00 through July 17 at 5:00.The most favourable Magnetic cloud occurred on July 15, 2012, between 19:00 and 06:00 UT. The shock on July 15, 2012, was another instance of an extremely geo-powerful shock happening inside a CME (Liu et al., 2014). According to the radiation belt estimations from the Van Allen Tests, there has been a significant decrease in the velocity of energetic particles in the external radiation belt.

The magnetic activity of the 23rd solar cycle was greater than the 24th solar cycle at the time of observation, according to Tripathy et al. (2015). As a result, the number of CMEs was higher than during the 24th solar cycle. Despite a 40 percentage reduction in sunspot numbers, Gopalswamy et al.

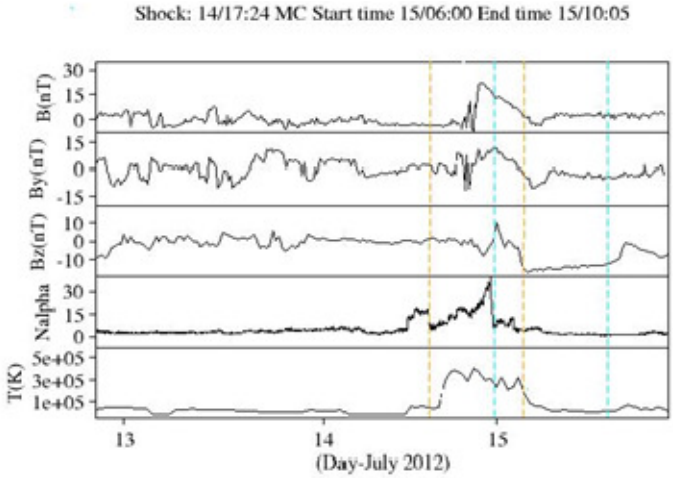

Fig. 2. ICME observed by ACE following the IP shock on 15 July 2012.

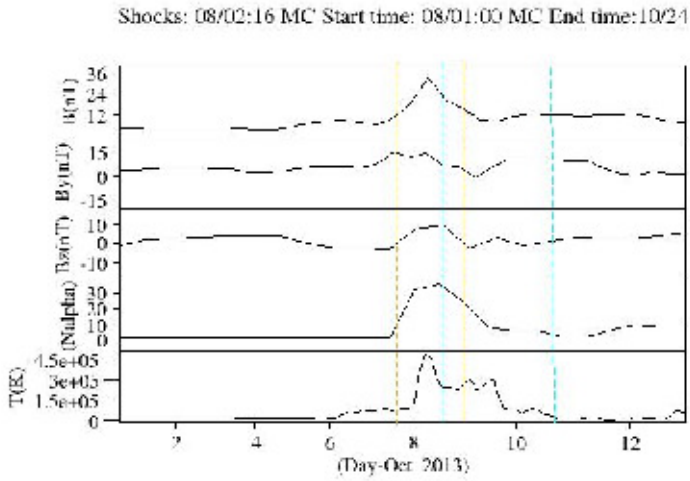

Fig. 3. ICME observed by ACE following the IP shock on 08 Oct. 2013.

Table 3. Disk center MC Events during the three phases of solar cycle 24

Phase	CME			
	Date	Time(UT)	V(km s^{-1})	MPA(deg)
Rising phase	02/07	0354	421	113
	02/12	1342	509	44
	03/07	2000	2125	313
	06/05	2205	2425	300
	08/05	0412	1315	298
	09/09	2305	575	300
	09/26	1248	1915	78
	10/25	1200	570	54
	11/29	1400	455	100
	11/29	1312	1064	134
Maximum phase	06/17	1412	987	144
	07/15	0624	873	329
	09/03	0400	538	90
	03/07	0712	1063	112
	10/02	0709	964	110
	10/08	1443	567	10
	11/09	1700	532	253
	12/08	0736	1085	274
	02/16	1000	634	227
	04/06	2312	514	115
	08/20	1112	600	359
	09/12	1800	1267	175
	12/23	1212	669	189
	03/17	0148	719	240
	09/20	1812	1239	219
Declining phase	07/19	0312	331	291
	07/19	1325	607	357
	10/12	0224	179	38
	09/08	1200	1385	72
	06/30	1248	185	261
	05/16	0912	305	79

(2015) observed that the rate of halo CMEs has increased during cycle 24 compared to cycle 23. It is crucial to remember that extraordinary occurrences can occur on 15 July 2012, with a magnetic field of -52nT and a speed of 1500 km s^{-1}, as a result of the greatest storm of solar cycle 24, which struck from 13 to 15 July 2012.

During the event, the magnetic field (Bz) is amplified and rotates smoothly. The blue vertical faint lines represent the magnetic clouds, and the orange vertical solid lines show the shock's arrival time at 1 AU. The ejecta were positioned at the conclusion of the study to allow for the measurement of the ICME interval. Two examples of ICMEs that induce shocks are shown in Fig. 2: on June 15, 2012, at 6:00 UT, an MC. The Tp depression is our main determinant of the ICME limitations. There are only two hours between our end time and the time of this report. It's intriguing to observe that most of the indications were present on June 15, 2012, up until about 6:00 UT, indicating

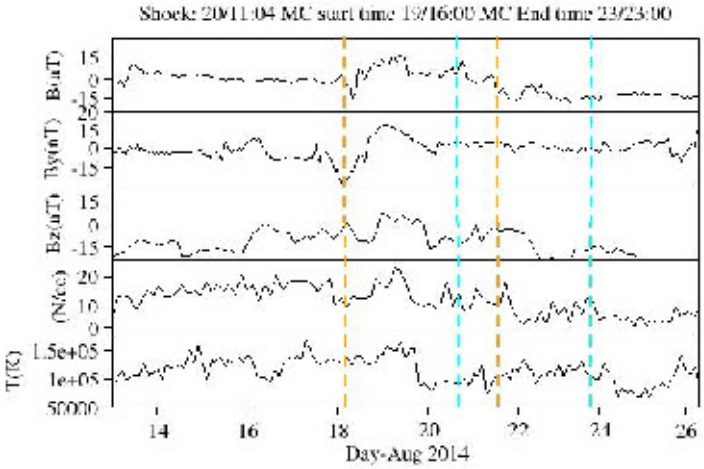

Fig. 4. Example of an ICME observed by ACE following the IP shock on 20 August 2014.

that further ejecta occurred after this MC event. For disk-centre events, the number of MCs is lowest during the rising phase and highest during solar maximum. The enhanced solar activity during solar maximum is the direct cause of this. A thorough examination of the five disk-centre CMEs linked to the solar origins of IP shock was provided by Gopalswamy 2010.

The entire magnetic field, Bx, which is roughly depicted in Fig. 2, abruptly spikes during the leading shock, which is how you can identify it. The in situ measurements and the computer operate essentially simultaneously. The peak values of velocity, total magnetic field, temperature, and density are remarkably close to the genuine values during the peak time. A rough estimate of the shocks passage time of 48 hours is also provided.

A decrease in magnetic field and a lower than expected proton temperature are indicators of the presence of the ICME magnetic cloud (Cane & Richardson, 1995, 2003). As it gets colder, the magnetic cloud starts to form. The magnetic cloud started on July 15, 2012, at 6:00 UT, according to this graph. The maximum plasma temperature that has been recorded throughout the time period under consideration is known as the maximum temperature. When the solar wind enters the heliosphere at a radial velocity faster than the solar wind it is going through, the solar wind is compressed on the leading edge of an ICME. The temperature increase during this compression is probably due to temperature gains along the leading edge of the ICME, which rely on the proton density and magnetic field (Light et al., 2020).

2.4 The Shock arrival time at 1 AU on 15 July 2012

Based on in-situ measurements, the shock's arrival time at 1 AU is shown by the blue-vertical solid lines (Mostl et al., 2014; Hess & Zhang, 2014). On July 14, at 17:24 UT, a shock and sheath area arrive at 1 AU simultaneously. The sheath region ended on July 15 at about 06:00 UT, and a magnetic cloud

started (Mostl et al., 2014). The shock arrival time from the simulation was only a little over an hour sooner than the data.

2.5 ICME and MC event on 08 Oct 2013

The ICME shock's surface position is S15 W12, and it occurred between 20:20 on October 8 and 00:00 on October 11.Between 0:00 and 24:00 on October 8, 2013, the magnetic cloud was more active. On October 8, 2013, the IP Shock occurred, causing the MC value to increase to a new peak. There aren't many active locations during solar minimum, and the filament disappearances take place around the equator. It has also been demonstrated that CMEs that are in close proximity to the solar minimum are frequently directed equatorially by the rapid solar wind flow that originates from huge pole coronal holes (Cremades & Bothmer, 2004). This shows that the majority of solar minimum CMEs, which have an MC structure, intersect the axis of the Earth. The majority of filament eruptions that take place at high latitudes during the solar optimum are either completely undeflected or mistakenly directed towards the poles (Cremades & Bothmer, 2004).

The magnetic field (Bz) is strengthened and rotates smoothly during the event. The magnetic clouds are depicted by the blue vertical faint lines, while the orange vertical solid lines indicate when the interplanetary shock will arrive. The list includes shocks generated by either MC shocks or IP shocks between December 2008 and December 2019. Each ICME's corresponding CME is monitored by the LASCO instrument on board the SOHO mission. The collected ICMEs are listed in Table 1 (MCs). Using information from Gopalswamy (2010), we divide the list of ICMEs in the declining phase into MCs.

MCs, which are among the most often used examples of ICMEs, are defined as ICMEs when the field intensity is high and the proton density and magnetic field are low mentioned by Bothmer & Schwenn (1998) and Sheeley et al. (1985). According to this diagram, interplanetary shocks start when the proton temperature starts to rise because as it does, so do the proton density and magnetic field. The IP Shock Event begins in this graph on October 7, 2013, at 20:24 UT. Ahead of them, shocks may be produced by ICMEs with sufficiently high proton temperatures in comparison to the background solar wind. Individual signatures, however, might not always be recognised in ICMEs (Cane & Richardson, 2003). An ICME may contain multiple signatures, but it does not mean that they are all coincident. When compared to other signatures, such as proton temperature depressions, some signs have been recorded comparatively infrequently (Cane & Richardson, 1995, 2003).

2.6 ICME and MC event on 20 August 2014

The surface position of the ICME shock in August 2014 was S17 W10, and it occurred between August 19 and August 21, both at 7:00 am. A long magnetic cloud lifetime is noticed on August 20, 2014. The results are a 440 $\mathrm{km\,s^{-1}}$ (nine hours) and 16:30 UT (August 20, 2014) ICME appearance time and speed at 1 AU. IP Shock's high peak first emerged on August 20, 2014. Activities for ICME and MC on August 20, 2014. ICME and MC activities on August 20, 2014. The more active MC and IP shock on August 20, 2014, are depicted in

this graph. The data for the magnetic field Bx, By, Bz, proton density Nalpha, and proton temperature Tp used in this graph were obtained from the ACE satellite. The IP shock occurs between August 19 at 11 o'clock and August 21, 2014. The IP shock can be seen as an orange line. One of the biggest shock peaks has occurred in solar cycle 24. The magnetic field (Bz) is strengthened and rotates smoothly during the event. The magnetic cloud's arrival time is shown by the blue vertical faint lines and the IP shocks by the orange vertical solid lines. The largest peak occurred during the Sun's maximum phase, when it is at its most active. As the sun's temperature rises, its activity rises as well. If the Sun is more active, the proton temperature increases, the IP shock intensifies, and on August 20, 2014, when this particular event is moving at a speed of 860 to 960 $\mathrm{km\,s^{-1}}$, a more active and long-lasting MC forms. The wider CMEs in a slower background solar wind (McComas et al., 2013) may be subject to more drag in the IP medium, resulting in a slower MC speed at 1 AU, which is one explanation. In cycle 24, there are also fewer MCs that are shock drivers.

This graph depicts the MC that existed between August 18 and August 22, 2014. The proton temperature is quickly falling during that time. Since solar wind plasma and magnetic field data have been easily accessible since the dawn of the space age, the low solar wind proton temperature zones are suitable starting points for an ICME list for this ACE mission. We utilise the criterion of abnormally low proton temperature as the major ICME identification signature since we are interested in detecting all sorts of ICMEs (Richardson & Cane, 1993).

Conclusion

This article presents an in-depth analysis of the solar parameters, CMEs, and ICMEs that happened from 2008 to 2019. The 24th solar cycle's declining phase took place between 2016 and 2019, its ascending phase between 2012 and 2015, and its ascending and maximum phases between 2009 and 2012. Between the end of 2012 and the beginning of 2013, Solar Cycle 24 reached its highest peak.

There are 208 ICME events in total and 255 MCs in the current work. We have looked into the interactions between CMEs and MCs and IP shocks as they are observed by the LASCO instruments on board the SOHO spacecraft. The ICME catalogue is produced using a different methodology than other catalogues.

According to the study's analysis of current data, the 23rd solar cycle's CME number is higher than the 24th solar cycle's. The MC event happened during the Maximum period. As evidenced by two geomagnetic storms, the determined shock, and the MC, CMEs usually involve two subsequent collisions. Here, we report two cases where two successive impacts were blended into one, leading to a particularly unpleasant geomagnetic effect on an average strength driver. This kind of driver (consistent, increasing Bz) combines the traits of shocks and CMEs. The shock on July 15, 2012, had a number of ICME and shock features, as well as IP conditions. This result raises the possibility that fluctuations in the ICME's magnetic field with respect to the observer at 1 AU may be to blame for variations in the structure that have been observed between MC occurrences.

References

Bothmer, V., & Schwenn, R., 1998, *Ann. Geophysicae*, 16, 1-24
Brueckner, G. E., Howard, R. A., Koomen, M. J., et al., 1995, *Solar Physics*, 162, 357-402
Cane, H.V., & Richardson, I., 1995, *J. Geophys. Res.*, 100 (A2), 1755-1762
Cane, H.V., & Richardson, I., 2003, *J. Geophys. Res.*, 108 (A4), 1156
Chi, Y., 2016, *Solar Physics*, 291, 2419-2439
Cremades, H., & Bothmer, V., 2004, *Astron. & Astrophys.*, 422(1), 307-322
Gopalswamy, N., 2010, *Proceedings of the 20th National Solar Physics Meeting*, held 31 May - 4 June, 2010 in Papradno, Slovakia, p. 108-130
Gopalswamy, N., Akiyama, S., Yashiro, S., et al., 2008, *Journal of Atmospheric and Solar Terrestrial Physics*, 70(2-4), 245-253
Gopalswamy, N., Makela, P., Xie, H., Akiyama, S. & Yasshiro, S., 2010, *AIP Conf. Proc.*, 1216, 452-458
Gopalswamy, N., Yashiro, S., Xie, H., et al., 2015, *J. Geophys. Res.*, 120(11), 9221
Hess, P., & Zhang, J., 2014, *ApJ*, 792, 49
Huttunen, K.E.J., Schwenn, R., Bothmer, V., & Kooskinen, H.E.J., 2005, *Ann. Geophysicae*, 23, 625-641
Lepping, R. P., Wu, C.-C., & Berdichevsky, D. B., 2015, *Solar Physics*, 290, 553–578 comparison of magnetic cloud parameters, sunspot number, and interplanetary quantities for the first 18 years of the wind mission,
Light, C., Bindi, V., Consolandi, C., et al., 2020, *ApJ*, 896, 133
Liu, Y. D., Luhmann, J. G., Kajdič, P., et al., 2014, *Nature Communications*, 5(1), 3481
McComas, D. J., Angold, N., Elliott, H. A., 2013, *ApJ*, 779, 2
Möstl, C., Amla, K., Hall, J. R., et al., 2014, *ApJ*, 787(2), 119
Munro, R. H., Gosling, J. T., Hildner, E., et al., 1979, *Solar Physics*, 61, 201-215
Richardson, I., & Cane, H. V., 1993, *J. Geophys. Res.*, 98(A9), 15295-15304
Richardson, I., & Cane, H. V., 2010, *Solar Physics*, 264, 189-237
Sheeley Jr., N. R., Howard, R. A., Koomen, M. J., et al., 1985, *J. Geophys. Res.*, 90(A1), 163-176
Song, H., & Yao, S., 2020, *Science China Technological Sciences*, 63 (11), 2171-2187
Stone, E. C., Frandsen, A. M., Mewaldt, R. A., et al., 1998, *Space Sci. Rev.*, 86(1-4), 1-22
Tripathy, S. C., Jain, K., & Hill, F., 2015, *ApJ*, 812, 20
Wu, C. C., & Lepping, R. P., 2011, *Solar Physics*, 269, 141-153
Zurbuchen, T. H., & Richardson, I., 2006, *Space Sci. Rev.*, 123, 31-43